Nonresonant enhancement of spontaneous emission in metal-dielectric-metal plasmon waveguide structures

Y. C. Jun, R. D. Kekatpure, J. S. White, and M. L. Brongersma[*]

Geballe Laboratory for Advanced Materials, 476 Lomita Mall, Stanford, California 94305, USA

We theoretically investigate the spontaneous emission process of an optical, dipolar emitter in metal-dielectric-metal slab and slot waveguide structures. We find that both structures exhibit strong emission enhancements at nonresonant conditions, due to the tight confinement of modes between two metallic plates. The large enhancement of surface plasmon-polariton excitation enables dipole emission to be preferentially coupled into plasmon waveguide modes. These structures find applications in creating nanoscale local light sources or in generating guided single plasmons in integrated optical circuits.

Understanding the interactions between single emitters and surrounding electromagnetic fields has been of great importance for both fundamental studies and device applications. Coherent interactions between atoms and fields provide an ideal test bed for studying fundamental aspects of quantum mechanics,[1,2] while the large enhancements of spontaneous emission (SE) in resonant cavities have enabled more efficient light emitting devices, drastic reductions in the threshold of lasers, and high efficiency single photon sources.[3,4] In addition to the many studies of sophisticated dielectric cavity and waveguide systems, there have been a number of investigations on SE enhancement near simple metallic structures such as metallic films[5,6] or nanoparticles.[7,8] These structures exploit the large density of states at the surface plasmon (SP) resonance frequency to achieve large emission enhancements. However, these resonant enhancements are limited by the narrow bandwidth and large metal losses around the SP resonance frequency. Recently, it was pointed out that the SE of a single emitter near a metallic nanowire can be enhanced away from the SP resonance in the limit of vanishing nanowire radius, enabling exciting new quantum optics experiments.[9,10] These pioneering experiments have stimulated an intense search for the best possible plasmonic structure geometries that enable efficient coupling of emitters to surface plasmon-polariton (SPP) modes and facile integration into complex, functional devices.

In this Brief Report, we present another approach to obtain large SE enhancements, based on SPP generations in metal-dielectric-metal (MDM) *slab* (2D) and *slot* (1D) waveguide structures (Fig. 1). Both structures are shown to exhibit strong emission enhancement due to the tight confinement of modes between two metallic plates at nonresonant wavelengths, resulting in preferential coupling of the dipole emission into SPP waveguide modes. In nonresonant regions, propagation lengths of SPP modes become longer. Additionally, MDM structures can be reproducibly fabricated and integrated with other chip-scale components. Such structures can thus be useful for building efficient on-chip light sources for integrated optics. Coupling the emission of single emitters to a well-defined waveguide mode may be also useful for generating and guiding single plasmons (or single photons) in an optical circuit.

A MDM slab [Fig. 1(a)] supports one fundamental transverse magnetic (TM) mode (also called the gap SPP mode) for sufficiently small gap sizes ($\sim$ order of tens of nanometers).[11,12] Because the electric field inside the gap is primarily directed normal to the metal surfaces, we expect that only a dipole oscillating normal to the metal surfaces will strongly couple to this mode. The SE enhancement factor F_P of such a dipole in the gap can be obtained by considering the work done on the dipole by its own reflected field,[13–15]

$$F_P = \frac{\gamma_\perp}{\gamma_0} = \frac{3}{2}\text{Im}\int_0^\infty \frac{(1 - r_{12}^P e^{i\phi_{12}})(1 - r_{13}^P e^{i\phi_{13}})}{(1 - r_{12}^P r_{13}^P e^{i\phi_{12}} e^{i\phi_{13}})}\frac{u_\parallel^3}{\ell_1}du_\parallel, \quad (1)$$

where the indices 1,2,3 indicate the dielectric and two semi-infinite metal regions. The decay rate of a normal dipole
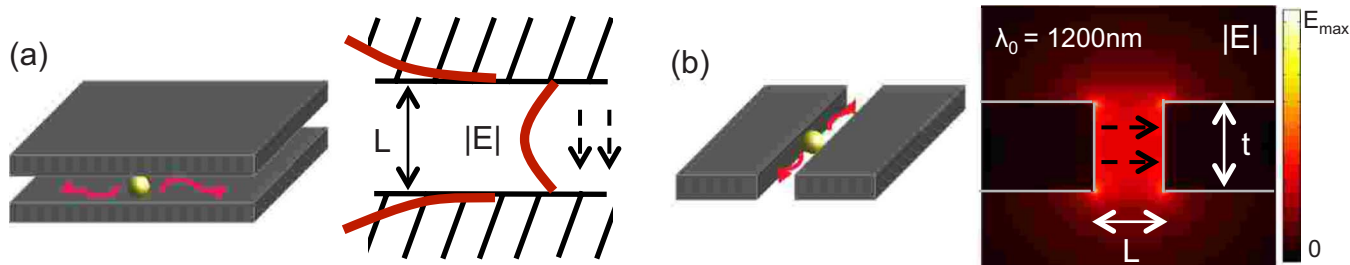

FIG. 1. (Color online) Schematic of metal-dielectric-metal (a) slab and (b) slot waveguides and electric field profile (|E|) of their fundamental modes. Dotted arrows indicate electric field directions inside the gaps. In (a), two semi-infinite metal plates are separated by a dielectric region of width L. In (b), two thin metal plates of thickness t are separated by a distance L and embedded in a uniform dielectric. The metal is silver and the dielectric has $\varepsilon_{\text{dielectric}}=2.25$.
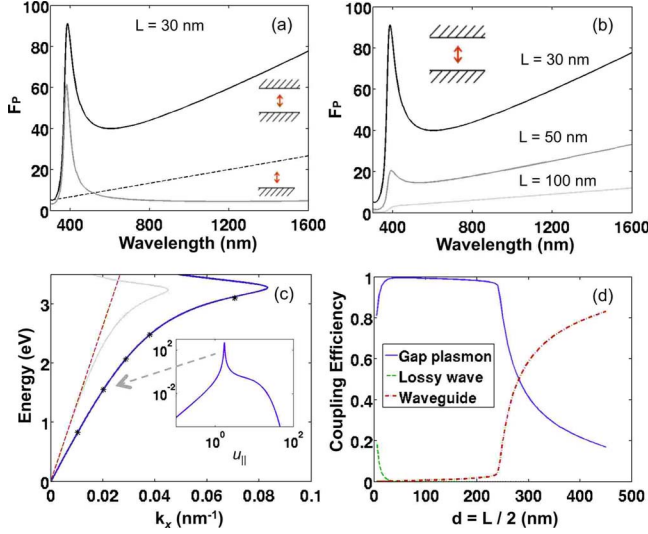
FIG. 2. (Color online) Spontaneous emission enhancement factor as a function of free-space wavelength (λ_0) (a) for a MDM structure vs a single metal-dielectric interface, and (b) for a MDM structure with different gap sizes. (c) Dispersion relation of the gap plasmon mode for $L=30$ nm (blue line), and the dispersion of a single silver surface (light gray line) and light line (dotted red line). Inset: decay rate density as a function of normalized in-plane wave vector. (d) Fraction of dissipated energy to each decay path as a function of metal-emitter distance d at $\lambda_0=800$ nm.

($\gamma_\perp$) is normalized to that in a uniform background dielectric medium (γ_0). Equation (1) is derived from a plane-wave decomposition of the emitted waves and $u_\parallel = k_\parallel/k_1$, $\ell_1 = -i(1-u_\parallel^2)^{1/2}$ correspond to their normalized in-plane and out-of-plane wave vectors. The Fresnel reflection coefficients (r_{12}^P, r_{13}^P) are multiplied by the corresponding round-trip phase changes ($e^{i\phi_{12}}$, $e^{i\phi_{13}}$).[16] The frequency-dependent dielectric constant of metal is obtained from the literature[17] and we assume internal quantum efficiency $\eta_0=1$ for the emitter.

Figure 2 shows the calculated SE enhancement factor as a function of the free-space wavelength for a dipole in the center of the gap, where the fields are exactly perpendicular to the metal surfaces. In addition to a resonant enhancement peak around 400 nm (which is close to SPP resonance wavelength of silver), there is strong nonresonant enhancement which increases linearly with wavelength [Fig. 2(a)]. For comparison, the SE enhancement factor for an emitter spaced by the same distance from a single metal surface is shown as well, which clearly lacks such nonresonant enhancement. We also observe that as the gap size decreases, both resonant and nonresonant enhancements increase rapidly [Fig. 2(b)]. To identify what causes these enhancements, a plot of the decay rate density [which is the integrand of Eq. (1)] as a function of normalized in-plane wave vector is shown [inset of Fig. 2(c)]. We find that decay rate density spectra for MDM slabs are dominated by single peaks with wavelength-dependent peak locations. By plotting the positions of these peaks (stars) along with the gap SPP mode dispersion curve, it can be seen that these peaks lie exactly on the curve [Fig. 2(c)]. The decay rate density also has contributions from broad, large wave vector components, so-called "lossy surface waves" (LSW) that originate from intrinsic metal losses.[14]
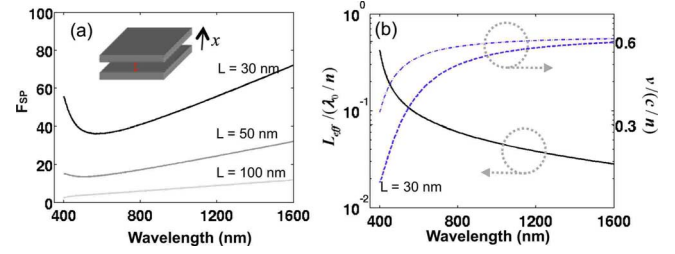

FIG. 3. (Color online) (a) Emission enhancement factor for a MDM slab (due to the gap SPP excitation) as a function of λ_0. (b) Normalized group velocity (dashed line), phase velocity (dashed-dotted line), and mode length (solid line) for $L=30$ nm.

By integrating the relevant wave vector regions, we can obtain the fraction of energy coupled into the gap SPP mode among three different decay channels: gap SPP, LSW, and the conventional TM waveguide mode. Figure 2(d) shows that gap SPP excitation is the dominant decay channel in a MDM slab for a wide range of metal-emitter distances at the considered nonresonant wavelength. We also note that when the metal-emitter distance becomes larger than ~250 nm, the fraction of gap SPP excitation decreases due to higher-order TM waveguide modes (which are similar to conventional waveguide modes).

To understand the physical origin of the behaviors observed in Fig. 2, we derive a simple analytical formula for SE enhancement for a dipole inside the gap of a MDM slab. From Fermi's golden rule, the SE rate of an emitter is given by $\gamma(x_e, \omega) = 2\pi|g(x_e,\omega)|^2 D_{2D}(\omega)$, where $|g|$ is the coupling strength between the dipole and the electromagnetic field at the emitter position x_e, and D_{2D} is the density of states. Assuming the dipole d_0 is oscillating normal to the metal surfaces, the coupling strength is given by

$$|g(x_e,\omega)|^2 = |\vec{d}_0 \cdot \alpha\vec{E}(x_e,\omega)/\hbar|^2 = \omega|\vec{d}_0|^2/(2\hbar\varepsilon\varepsilon_0 V_{\text{eff}}),$$

where $|\alpha|^2 = \hbar\omega/\int_{-\infty}^{\infty}\{\varepsilon_0 d(\varepsilon\omega)/d\omega|E|^2 + \mu_0|H|^2\}dx$ is a normalization factor. We define the effective mode volume $V_{\text{eff}} = L_{\text{eff}} \cdot \ell^2$, where ℓ is an arbitrary quantization length and L_{eff} is the effective mode length across the gap:

$$L_{\text{eff}}(x_e,\omega) = \frac{1}{2}\int_{-\infty}^{\infty}\left\{\varepsilon_0\frac{d(\varepsilon\omega)}{d\omega}|E(x,\omega)|^2 \right.$$
$$\left. + \mu_0|H(x,\omega)|^2\right\}dx/(\varepsilon\varepsilon_0|E(x_e,\omega)|^2).$$

The density of states can be obtained by counting modes in a 2D space, and is given by $D_{2D}(\omega) = \ell^2\omega/[2\pi v_p(\omega)v_g(\omega)]$, where v_p and v_g are the phase and group velocities, respectively. By normalizing the SE rate with that in a uniform background medium, we arrive at the expression for the SE enhancement factor due to the gap SPP excitation:

$$F_{\text{SP}} = \frac{\gamma_{sp}}{\gamma_0} = \frac{3}{4}\cdot\frac{c/n}{v_p}\cdot\frac{c/n}{v_g}\cdot\frac{\lambda_0/n}{L_{\text{eff}}},\qquad (2)$$

where $\gamma_0(\omega) = \omega^3\sqrt{\varepsilon}|d_0|^2/(3\hbar\pi\varepsilon_0 c^3)$. Figure 3 shows the calculated enhancement factor F_{SP} as a function of wavelength. We find that Fermi's golden rule calculation retrieves the

result of the analytical solutions well. Near the surface plasmon resonance, v_p and v_g rapidly decrease and thus F_{SP} exhibits a peak. In the nonresonant region, the velocity reductions are small, but the normalized mode length $L_{eff}/(\lambda_0/n)$ decreases steadily with wavelengths due to the tight confinement of modes between the two metal plates, giving rise to substantial nonresonant enhancements. This is in contrast to a single metal surface which confines the mode tightly only near the SPP resonance frequency. As the gap size is decreased, v_p, v_g, and L_{eff} all decrease, thus giving larger enhancements. Equation (2) also explains the difference between real metal and ideal perfect electrical conductor (PEC). The plasmonic response of real metal reduces v_p and v_g, which results in larger enhancement than that of PEC MDM [dotted line in Fig. 2(a)].

Strong SE enhancement can also be achieved with MDM slot structures which are more compatible with large scale integration. Recently, it was shown that slot structures (with critical dimensions on the order of tens of nanometers) support broadband and highly confined plasmonic modes—even into the long infrared (IR) regime.[18,19] In order to quantify the attainable enhancement, we first obtain the eigenmodes of slot waveguides with COMSOL finite element simulations [Fig. 1(b)]. We find that the mode is tightly confined around the slot and the electric field inside the gap is primarily directed normal to the metal slot surface. Therefore, we expect that this slot waveguide structure can also support nonresonant enhancement for a dipole oriented normal to the metal surfaces. We derive a similar analytical formula for the SE enhancement factor in slot waveguides. The coupling strength is given by the same expression $|g|^2 = \omega|d_0|^2/(2\hbar\varepsilon\varepsilon_0 V_{eff})$, but now we define the effective mode volume as $V_{eff}=A_{eff}\cdot\ell$, where the effective mode area is

$$A_{eff}(\vec{r}_e,\omega) = \frac{1}{2}\int\int\left\{\varepsilon_0\frac{d(\varepsilon\omega)}{d\omega}|E(\vec{r},\omega)|^2 + \mu_0|H(\vec{r},\omega)|^2\right\}d\vec{r}/(\varepsilon\varepsilon_0|E(\vec{r}_e,\omega)|^2).$$

Assuming a 1D density of states $D_{1D}(\omega)=\ell/[\pi v_g(\omega)]$, we find the emission enhancement due to the slot mode excitation to be

$$F_{SP} = \frac{\gamma_{sp}}{\gamma_0} = \frac{3}{4\pi}\cdot\frac{c/n}{v_g}\cdot\frac{(\lambda_0/n)^2}{A_{eff}}. \tag{3}$$

From COMSOL finite element simulations, we solved for the group velocity and mode area of slot eigenmodes for three different metal film thicknesses [Fig. 4(b)] with a fixed gap size. The calculated enhancement factors [Fig. 4(a)] show that the simple slot structures exhibit strong nonresonant enhancements due to a large mode area reduction. Additionally, we see that as the film gets thinner, the enhancement increases due to both group velocity and mode area reductions.

To verify our results, full-field 3D finite-difference time domain (FDTD) simulations were used, which include all possible decay pathways. The enhancement factor can be obtained by calculating the power dissipated by a dipole in the center of a MDM slot and in free space: $F_P = \gamma/\gamma_0$
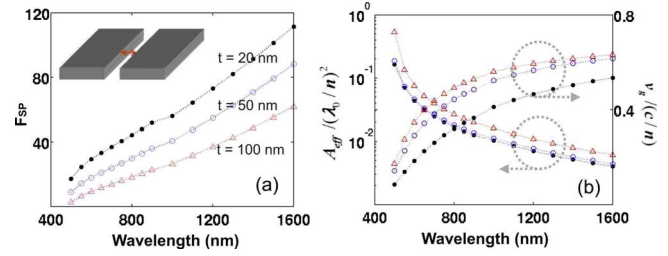

FIG. 4. (Color online) (a) Emission enhancement factor for a MDM slot (due to the slot mode excitation) as a function of λ_0 for different metal thicknesses, and $L=40$ nm. (b) Normalized group velocity and mode area (solid circle: $t=20$ nm, open circle: $t=50$ nm, open triangle: $t=100$ nm).

$=\langle P\rangle/\langle P_0\rangle$, where $\langle P(t)\rangle = \omega/2\,\text{Im}\{\vec{d}_0\cdot\vec{E}(r_e)\}$.[14] First, as a validity check, the result of 3D FDTD calculations are compared to the analytic case of an infinite thickness slot (i.e., MDM slab) [Fig. 5(a)]. The FDTD calculation retrieves the analytic results in both resonant and nonresonant regions, although it is slightly overestimated, likely due to the finite space discretization of 2 nm used in the simulations. 3D FDTD calculations were performed for MDM slots of three different metal film thicknesses [Fig. 5(b)]. From the simulated profile of the Poynting vector, it can be clearly seen that a bound mode is launched into the slot direction [inset of Fig. 5(b)]. The fraction of energy coupled to the slot mode can be estimated more directly through 3D FDTD flux calculations. By measuring the flux into the slot direction and normalizing it to the total power flux, the coupling efficiency to the slot mode can be determined.[20] For $L=40$ nm and $t=50$ nm, we find the slot mode coupling efficiencies are ~ 80–90% at the considered nonresonant wavelengths.

In the nonresonant regime, the electromagnetic field penetrates less into the metal and the propagation lengths of the plasmon modes in both MDM slab and slot structures rapidly increase with wavelength.[11,12] Consequently, the large nonresonant enhancement is a desirable feature for optical device applications involving SPP modes. Moreover, in the nonresonant regime, MDM structures confine the electromagnetic mode mainly in the dielectric region between the metal plates, enabling direct conversion of the SPP mode to a
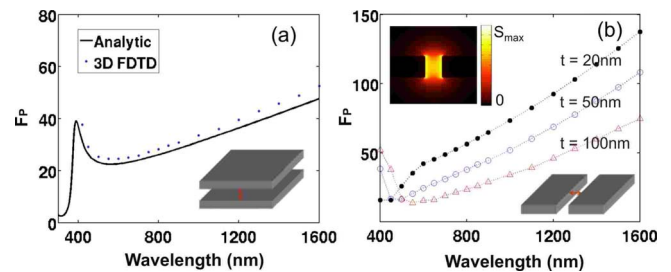

FIG. 5. (Color online) (a) Spontaneous emission enhancement factor for a MDM slab. 3D FDTD results are compared to the analytical solution. (b) Spontaneous emission enhancement factor for a MDM slot (calculated from 3D FDTD simulation for three different metal thicknesses, and $L=40$ nm). Inset: Poynting vector profile ($|\langle S\rangle|$) calculated 600 nm away from the source dipole (for $t=50$ nm and $\lambda_0=1200$ nm).

conventional dielectric waveguide mode through proper coupler structures.[21,22] By combining these out-coupling structures with MDM waveguides, MDM structures can be used for on-chip, local light sources in highly integrated optical systems.

Coupling the emission of single emitters to a slot waveguide could enable efficient ways to generate and guide single plasmons[9,10] on an integrated optical circuit, which can be also converted to single photons in free space or in a dielectric waveguide. MDM slots can be fabricated reproducibly with standard nanofabrication techniques (such as focused ion beam) and can be easily integrated with other components. The broadband nature of these structures makes spectral tuning unnecessary, thus removing stringent fabrication requirements to get reproducible emission enhancements. Additionally, the two separate metal plates of MDM structures can be used for electrical contacts and may enable tunable single photon emission or switching by applying electric fields to an emitter in the gap. Finally, MDM slot waveguides are also expected to be useful for studying the recently proposed nonlinear interactions of single photons via two-level[23] or three-level[24] atomic systems in a 1D waveguide.

In conclusion, we have shown that simple MDM waveguide structures can support strong emission enhancements over broad, nonresonant wavelength regimes. The resulting efficient coupling of emission to the plasmon mode makes MDM structures promising for both fundamental light-matter interaction studies and device applications.

*brongersma@stanford.edu

[1] E. A. Hinds, in *Cavity Quantum Electrodynamics*, edited by P. R. Berman (Academic, San Diego, CA, 1994).

[2] S. Haroche and D. Kleppner, Phys. Today **42**(1), 24 (1989).

[3] G. Bjork, Y. Yamamoto, and H. Heitmann, in *Confined Electrons and Photons*, edited by E. Burstein and C. Weisbuch (Plenum, New York, 1995).

[4] K. J. Vahala, Nature (London) **424**, 839 (2003).

[5] A. Neogi, C.-W. Lee, H. O. Everitt, T. Kuroda, A. Tackeuchi, and E. Yablonovitch, Phys. Rev. B **66**, 153305 (2002).

[6] K. Okamoto, I. Niki, A. Shvartser, Y. Narukawa, T. Mukai, and A. Scherer, Nature Mater. **3**, 601 (2004).

[7] J. Gersten and A. Nitzan, J. Chem. Phys. **75**, 1139 (1981).

[8] H. Mertens, A. F. Koenderink, and A. Polman, Phys. Rev. B **76**, 115123 (2007).

[9] D. E. Chang, A. S. Sorensen, P. R. Hemmer, and M. D. Lukin, Phys. Rev. Lett. **97**, 053002 (2006).

[10] A. V. Akimov, A. Mukherjee, C. L. Yu, D. E. Chang, A. S. Zibrov, P. R. Hemmer, H. Park, and M. D. Lukin, Nature (London) **450**, 402 (2007).

[11] R. Zia, M. D. Selker, P. B. Catrysse, and M. L. Brongersma, J. Opt. Soc. Am. A **21**, 2442 (2004).

[12] J. A. Dionne, L. A. Sweatlock, H. A. Atwater, and A. Polman, Phys. Rev. B **73**, 035407 (2006).

[13] R. Chance, A. Prock, and R. Silby, Adv. Chem. Phys. **37**, 1 (1978).

[14] G. W. Ford and W. H. Weber, Phys. Rep. **113**, 195 (1984).

[15] We focus our study on gap sizes of tens of nanometers, where the nonlocal response of metal is not considered critical to our electrodynamics calculations. For the nonlocal response of metal, see, e.g., Ref. 14.

[16] W. L. Barnes, J. Lightwave Technol. **17**, 2170 (1999).

[17] A. D. Rakic, A. B. Djurisic, J. M. Elazar, and M. L. Majewski, Appl. Opt. **37**, 5271 (1998).

[18] D. F. P. Pile, T. Ogawa, D. K. Gramotnev, Y. Matsuzaki, K. C. Vernon, K. Yamaguchi, T. Okamoto, M. Haraguchi, and M. Fukui, Appl. Phys. Lett. **87**, 261114 (2005).

[19] G. Veronis and S. Fan, J. Lightwave Technol. **25**, 2511 (2007).

[20] The flux into the slot direction decreases as away from the source, due to the metal loss. To compensate for this, the flux was measured as a function of distance to the source and fitted to an exponential function (e^{-x/L_P}) to get the undamped flux value, where L_P is the propagation length and x is the distance to the source.

[21] L. Chen, J. Shakya, and M. Lipson, Opt. Lett. **31**, 2133 (2006).

[22] G. Veronis and S. Fan, Opt. Express **15**, 1211 (2007).

[23] J. T. Shen and S. Fan, Phys. Rev. Lett. **98**, 153003 (2007).

[24] D. E. Chang, A. S. Sorensen, E. A. Demler, and M. D. Lukin, Nat. Phys. **3**, 807 (2007).